SUPPLEMENTAL MATERIAL

Supplemental methods:

All protocols for animal experiments were approved by the respective Institutional Animal Care and Use Committee (IACUC).

Animal Models:

8 to 12 weeks old female C57Bl/6J mice (Jackson laboratories, Bar Harbor, ME) were used for experiments. All procedures were performed under anesthesia with 1–3% isoflurane (Forane, Baxter, Deerfield, IL) and 0.1mg/kg s.c. Buprenorphine (Reckitt Benckiser Richmond, VA) BID. MI was induced with permanent coronary ligation model as described previously (1). Briefly, anesthetized mice were intubated, thoracotomy was performed in the left fourth intercostal space and the left coronary artery was permanently ligated. For ischemia reperfusion injury (IRI) model, left coronary artery was transiently ligated for 30 minutes and then the ligation suture was removed (2). For drug treatment, mice received 50mg/kg of PF-1355 dissolved in vehicle excipient containing 40mM Tris, 0.5% hydroxypropylmethylcellulose acetate succinate (HPMCAS) and 10% hydroxypropyl methylcellulose (HPMC), pH 10, twice daily by oral gavage (3). Most mice had the treatments started within 1 hour after infarct induction. A separate group had the treatments started 24 hours after infarct induction. Control infarcted mice received either vehicle treatment twice daily or no treatment as mentioned in the respective sections. Untreated MI controls were employed to better mimic the clinical scenario where control patients will not be administered with any excipient mixture. In separate experiments, vehicle treatment was also performed as a more robust comparison to PF-1355 therapy.

In Vivo Imaging

Day 2 MRI Imaging: To evaluate the effects of the MPO inhibitor PF-1355 noninvasively, mice were imaged with MPO-Gd (*bis*-5-hydroxytryptamide-diethylenetriaminepentaacetate-gadolinium) molecular MR agent on day 2 after MI and IRI. MPO-Gd is an activatable MR imaging agent that reports *extracellular* MPO activity *in vivo* with high specificity and sensitivity (4,5). MPO-Gd was synthesized in our laboratory as previously described (6). MR imaging was performed by using an animal 7-T MR imaging unit (Bruker, Billerica, MA) and custom-made cardiac birdcage coil (Rapid Biomedical, Wuerzburg, Germany) before and after intravenous administration of MPO-Gd (0.3 mmol/kg). Early and delayed T1-weighted images of the left ventricle were obtained in its short axis with ECG and respiratory gating. Gradient echo FLASH-sequences were used with following parameters: echo time (TE), 2.7ms; 16 frames per PR interval; flip angle 60 degrees; in-plane resolution 200×200μm; slice thickness 1mm. Contrast-to-noise ratio (CNR) of the infarct was measured as described previously (1) and *in vivo* MPO activation was reported as (i) CNR value at 60 minutes post contrast injection and (ii) by calculating the lesion activation ratio (LAR: ratio of CNR at delayed [60 minutes] to early [15 minutes] time points) (5). Early enhancement represents mostly nonspecific signal whereas delayed enhancement is derived from agent retention caused by MPO activation. The enhancing area was also quantified in a single mid-ventricular slice. Infarct size was quantified 2 days after MI by measuring MPO-positive areas on MPO-Gd MR images.

Day 21 MRI Imaging: To evaluate effects of PF-1355 on post-MI remodeling, treatment groups were divided into long and short treatment cohorts. The long treatment cohort (n=5) was treated for 21 days and then imaged with cine cardiac volumetric imaging. The short treatment cohort (n=8) was treated only for first 7 days post-MI (early healing phase), and then treatment was

stopped until day 21 imaging. Both cohorts underwent molecular MRI with MPO-Gd on day 2 to confirm infarct presence and MPO specific signal quantification. 6-8 short axes imaging slices were obtained spanning the infarcted left ventricle as described previously (7) to calculate ejection fraction (EF), end-diastolic volume (EDV) and left ventricular mass.

Echocardiography: Animals underwent transthoracic echocardiography before surgery and 4 weeks later after surgery. Animals were lightly anaesthetized with 1-1.5% isoflurane to maintain heart rate between 400 to 500 bpm, and imaged using a Vevo 770 ultrasound system (VisualSonics, Toronto, Canada) as previously described (8). M-mode images were acquired in the parasternal short-axis view at the level of the papillary muscle. LV internal dimensions were measured and the LV fractional shortening (FS) and LV ejection fraction (EF) were calculated.

MPO Activity Assay:

Mice were sacrificed 2 hours after the morning dose on day 2 post-MI, and hearts were processed further for extracellular (ECF) and intracellular (ICF) fractions as described previously (9). Briefly, mice were transcardially perfused with 20mL PBS containing 10U/mL of Heparin [APP Pharmaceuticals, Schaumburg, IL]. Hearts were harvested and incubated in ECF extraction buffer (0.32M sucrose [Sigma], 1 mM $CaCl_2$[Sigma], 10U/ml Heparin in Hanks Balanced Salt Solution [HBSS]). After 2 hours, hearts were homogenized, sonicated and centrifuged at 15,000g to obtain the ICF fraction. ECF extraction buffer was mixed with 4 parts ice-cold acetone (Fisher Scientific) and incubated for 1 hour at −20°C for protein precipitation. Resultant precipitate was pelleted, dissolved in PBS and protein concentration of the extracts was measured with bicinchoninic acid assay kit (BCA; Thermo Scientific, Waltham, MA).

To specifically capture MPO from mice infarcts, 40-50 µg of ECF and ICF samples were diluted in MPO ELISA dilution buffer and incubated in anti-MPO antibody coated plates (Hycult,

Plymouth Meeting, PA) for 1 hour at room temperature followed by washing. MPO activity of antibody-captured MPO was assessed with 10-acetyl-3,7-dihydroxyphenoxazine (ADHP, AAT Bioquest, Sunnyvale, CA) peroxidation assay and data was acquired on Safire 2 microplate reader (Tecan, Durham, NC) at an excitation wavelength of 535nm and an emission wavelength of 590nm (9).

Effect of PF-1355 on both purified human MPO (final conc. 0.06pM; Lee Bioscience, MO) and mouse MPO extracted from bone marrow neutrophils and heart infarct was quantified using ADHP peroxidation assay. Half maximal inhibitory concentration (IC_{50}) of PF-1355 was measured.

Murine Neutrophil Isolation

Murine bone marrow neutrophils were isolated as described (10) and processed further for MPO extraction to be used as positive control. Briefly, bone marrow cells were extracted by flushing with staining buffer (Dulbecco's phosphate buffered saline [DPBS] with 0.5% bovine serum albumin [BSA] and 1% fetal bovine serum [FBS]) and subjected to red blood cell (RBC) lysis according to manufacturer's instructions (Biolegend, San Diego, CA). Cells were centrifuged on a 0–62% discontinuous percoll (GE Healthcare, Little Chalfont, UK) gradient for 30 min at 1000g. Pellet containing neutrophils was harvested, washed and counted with hemocytometer and trypan blue (Mediatech, Inc.) dead cell exclusion. Cells were then processed similar to ICF tissue for extracting murine MPO.

Flow cytometry:

Flow cytometry was performed at days 2, 7, and 15 post-MI to quantify leukocyte subsets. Hearts were harvested and single cell suspensions were prepared as described previously (11). Briefly, hearts were minced and shaken for 1 hour at 37°C in a cocktail mix of 450U/ml collagenase I, 125U/ml collagenase XI, 60U/ml DNase I and 60U/ml hyaluronidase (Sigma-Aldrich, St. Louis, MO). Cells were passed through a cell 40 µm cell strainer, washed and resuspended in staining buffer for counting and antibody staining. Peripheral blood was also collected through cardiac puncture and RBC lysis was performed to purify leukocytes. Following antibodies were purchased from BD Bioscience unless otherwise indicated: anti-CD45-APC, 30-F11; lineage cocktail (anti-CD90-PE, 53-2.1; anti-NK1.1-PE, PK136; Anti B220-PE, RA3-6B2; anti-CD49b-PE, DX5; anti-TER-119-PE, TER-119); anti-CD11b-APC-Cy7, M1/70; anti-Ly-6C-FITC, AL-21; anti-F4/80-PE-Cy7, C1:A3-1 and biotin anti-Ly-6G, IA8 (BioLegend, San Diego, CA). A streptavidin-Pacific Orange conjugated secondary antibody was used for labeling biotinylated antibodies.

All Leukocytes were identified as the $CD45^{+}$, and myeloid cells as $(CD45^{+})(Lin^{low}\ CD11b^{high})$. Myeloid cells were further divided into neutrophils as $[(F4/80^{low})\ (Ly\text{-}6G^{high}\ Ly\text{-}6C^{int})(SSC^{int\text{-}high})]$, Ly-$6C^{high}$ monocytes as $[(F4/80^{low})(Ly\text{-}6G^{low}\ Ly\text{-}6C^{high})]$, and Ly-$6C^{low}$ monocytes as $[(F4/80^{low})(Ly\text{-}6G^{low}\ Ly\text{-}6C^{low})]$. Gating scheme utilized has been illustrated in **SI Fig. 5**. Cell numbers of different cell populations were calculated as total viable cells multiplied by the percentage of the respective sub-population. Data for different leukocyte subsets were also reported as the percentage of total leukocytes ($CD45^{+}$). Data were acquired on a flow cytometer (LSR II; BD Biosciences, San Jose, CA) and analyzed with dedicated software (FlowJo 887; Tree Star, Ashland, Ore).

Histology

Histopathology was performed on days 7 and 14 post-MI for assessing CD11b and MPO expressing cells as well as the effect of PF-1355 on infarct healing. Briefly, hearts were harvested, embedded in OCT compound (Sakura Finetek, PA) and freshly frozen in cold isobutane. Care was taken to remove air bubbles from the ventricular chambers also filled with OCT. Following antibodies were used for histopathology at the midventricular infarcted tissue sections: CD11b (clone M1/70, BD Pharmingen, San Diego, CA); anti-MPO (clone Ab-1, ThermoFisher Scientific, Waltham, MA); CD31 for endothelial cells (clone MEC13.3, BD Pharmingen) and collagen-1 (abcam, Cambridge, MA). Biotinylated secondary antibody ABC kit (Vector Laboratories, Inc., Burlingame, CA) and AEC substrate (DakoCytomation, Carpinteria, CA) was used for color development. Hematoxylin was used as a counter stain followed by the image capture with the NanoZoomer 2.0-RS (Hamamatsu). Positive areas were quantified as percentage of high power field (HPF) in 5-6 HPF/slice section/mouse by using IPLab (version 3.9.3; Scanalytics, Inc.) at magnification 100x to 400x.

On day 7, infarct wall thickness was measured in vehicle and PF-1355 treated groups post-MI by two different investigators blinded to the experimental groups. In a single midventricular slice, five to six representative wall areas per mouse were selected for averaging, starting from the infarct edges to the core. For each area, wall thickness at low magnification (50x) was measured by drawing a perpendicular line from epicardium to endocardium with the help of NanoZoomer 2.0-RS (Hamamatsu). Care was taken to avoid papillary muscles in selected areas.

Statistical Analysis

Results were reported as mean ± standard error of mean (SEM). D'Agostino & Pearson omnibus test was applied to ascertain data normality. If data groups were non-normal or when sample size was not large enough to calculate normality, we applied Mann-Whitney *U* test. In other cases, Student's *t* test was applied for independent group comparisons. One-way ANOVA with Tukey multiple comparisons was performed to compare >2 groups. $P<0.05$ was considered to indicate a significant difference. All statistical analyses were performed with GraphPad Prism 6, GraphPad Software.

Supplemental table:

Table-1: Day 2 PF-1355 plasma levels

Time (hours)	Gender	Mean plasma conc. (nM)	SD
2	Female	21184	5545
6	Female	5016	2536
14	Female	3146	2595

SI Table 1: PF-1355 plasma concentrations (nM) from animals (n=7-8 per time point). Plasma samples were taken at various time points (2, 6 and 14 hours) after the PF-1355 (50mg/kg) oral dosing at day 2 after MI. Plasma drug levels were measured as described previously.(3)

Supplemental references:

1. Nahrendorf M, Sosnovik D, Chen JW et al. Activatable magnetic resonance imaging agent reports myeloperoxidase activity in healing infarcts and noninvasively detects the antiinflammatory effects of atorvastatin on ischemia-reperfusion injury. Circulation 2008;117:1153-60.
2. Vasilyev N, Williams T, Brennan M-L et al. Myeloperoxidase-Generated Oxidants Modulate Left Ventricular Remodeling but Not Infarct Size After Myocardial Infarction. Circulation 2005;112:2812-2820.
3. Zheng W, Warner R, Ruggeri R et al. PF-1355, a mechanism-based myeloperoxidase inhibitor, prevents immune complex vasculitis and anti-glomerular basement membrane glomerulonephritis. The Journal of pharmacology and experimental therapeutics 2015;353:288-98.
4. Forghani R, Wojtkiewicz GR, Zhang Y et al. Demyelinating diseases: myeloperoxidase as an imaging biomarker and therapeutic target. Radiology 2012;263:451-60.
5. Breckwoldt MO, Chen JW, Stangenberg L et al. Tracking the inflammatory response in stroke in vivo by sensing the enzyme myeloperoxidase. Proc Natl Acad Sci U S A 2008;105:18584-9.
6. Chen JW, Querol Sans M, Bogdanov A, Jr., Weissleder R. Imaging of myeloperoxidase in mice by using novel amplifiable paramagnetic substrates. Radiology 2006;240:473-81.
7. Panizzi P, Swirski FK, Figueiredo JL et al. Impaired infarct healing in atherosclerotic mice with Ly-6C(hi) monocytosis. J Am Coll Cardiol 2010;55:1629-38.
8. Ram R, Mickelsen DM, Theodoropoulos C, Blaxall BC. New approaches in small animal echocardiography: imaging the sounds of silence. American journal of physiology Heart and circulatory physiology 2011;301:H1765-80.
9. Pulli B, Ali M, Forghani R et al. Measuring myeloperoxidase activity in biological samples. PLoS One 2013;8:e67976.
10. Preparation of mouse bone marrow neutrophils. Available: http://medicine.ucsf.edu/labs/brown/protocols_03_2005/Murine_BMN_Prep.pdf.
11. Nahrendorf M, Swirski FK, Aikawa E et al. The healing myocardium sequentially mobilizes two monocyte subsets with divergent and complementary functions. J Exp Med 2007;204:3037-47.

Supplemental figures and figure legends:

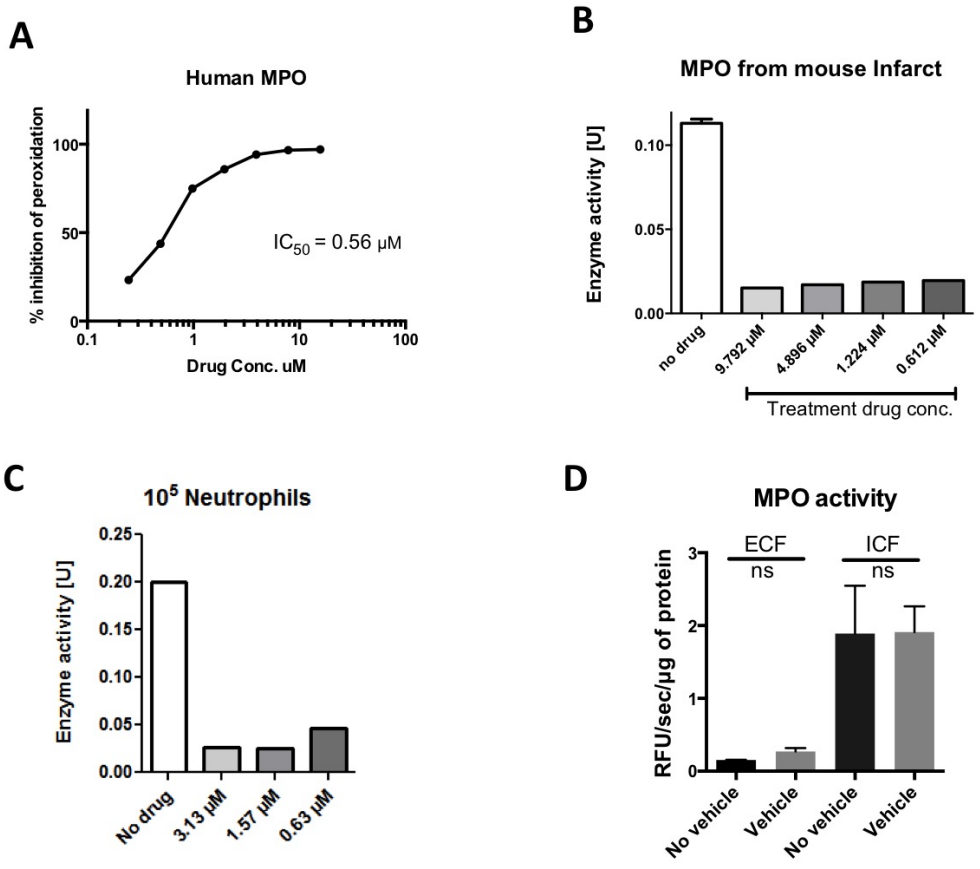

SI Fig. 1: (A) In vitro measurement of MPO inhibitory effect with pure human MPO protein. Serial dilutions of drug were added on 96 well plates without anti-MPO antibody capture and MPO peroxidase activity was measured with amplite ADHP, plotted as % inhibition compared to positive control without drug. IC_{50} was measured to be 0.56uM. (B) MPO inhibition of mouse MPO extracted from infarct by anti-MPO antibody capture assay. (C) MPO was extracted from mouse neutrophils. Equal volumes of neutrophil extract were loaded on 96-well plates and with three different concentrations of PF-1355 (grey bars). MPO activity was measured with anti-body capture assay with ADHP and compared to control neutrophil extract without drug (white

bar). (D) MPO activity in both the ECF and ICF fraction of vehicle treated mice was similar to the mice without any vehicle treatment (n=3-7, P = ns). IC_{50}: half maximal inhibitory concentration

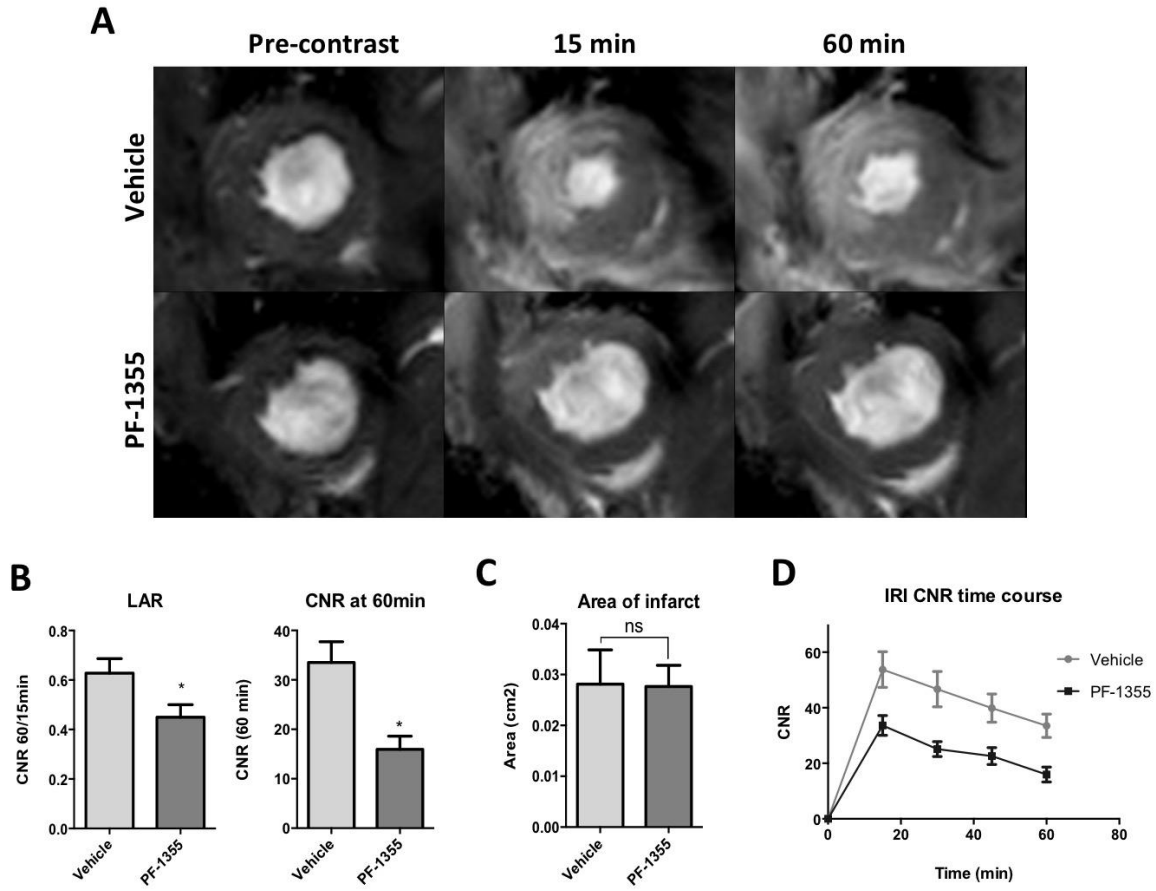

SI Fig. 2: PF-1355 inhibits MPO in ischemia reperfusion injury (IRI) model as imaged non-invasively by MPO-Gd imaging. (A) Representative T1-weighted mid-ventricle slices showing pre-contrast, early (15 min) and delayed (60 min) contrast enhanced images. (B) Lesion activation ratio (LAR) of vehicle (n=8) and PF-1355 treated groups (n=5) and bar graphs representing 60 min CNR values. (C) There is no significant difference in infarct area between groups at day 2 post-IRI. (D) CNR values plotted as a function of time represent decrease in enhancement as compared to vehicle treated controls. Data plotted as mean ± SEM; *P <0.05

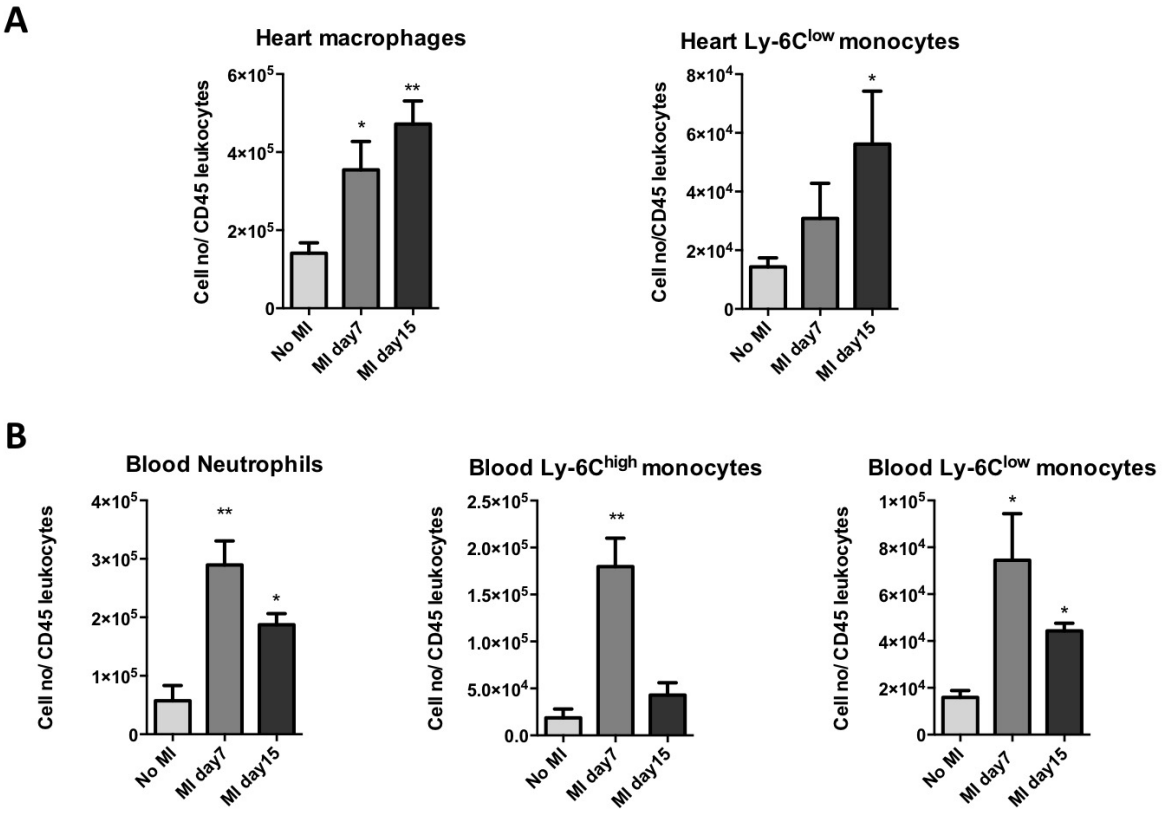

SI Fig. 3: (A) Heart macrophages and Ly-6C^{low} monocytes were significantly elevated at day 15 compared to no MI. Although not significant, a trend towards increased macrophages and Ly-6C^{low} monocytes was also seen at day 15 compared to day 7 (B) Bar graphs representing data from blood samples showed increased neutrophils, Ly-6C^{high} and Ly-6C^{low} monocytes/CD45^{+} leukocytes/ml of blood both at day 7 and day 15 as compared to no MI. Data plotted as mean ± SEM; *P <0.05; **P <0.01

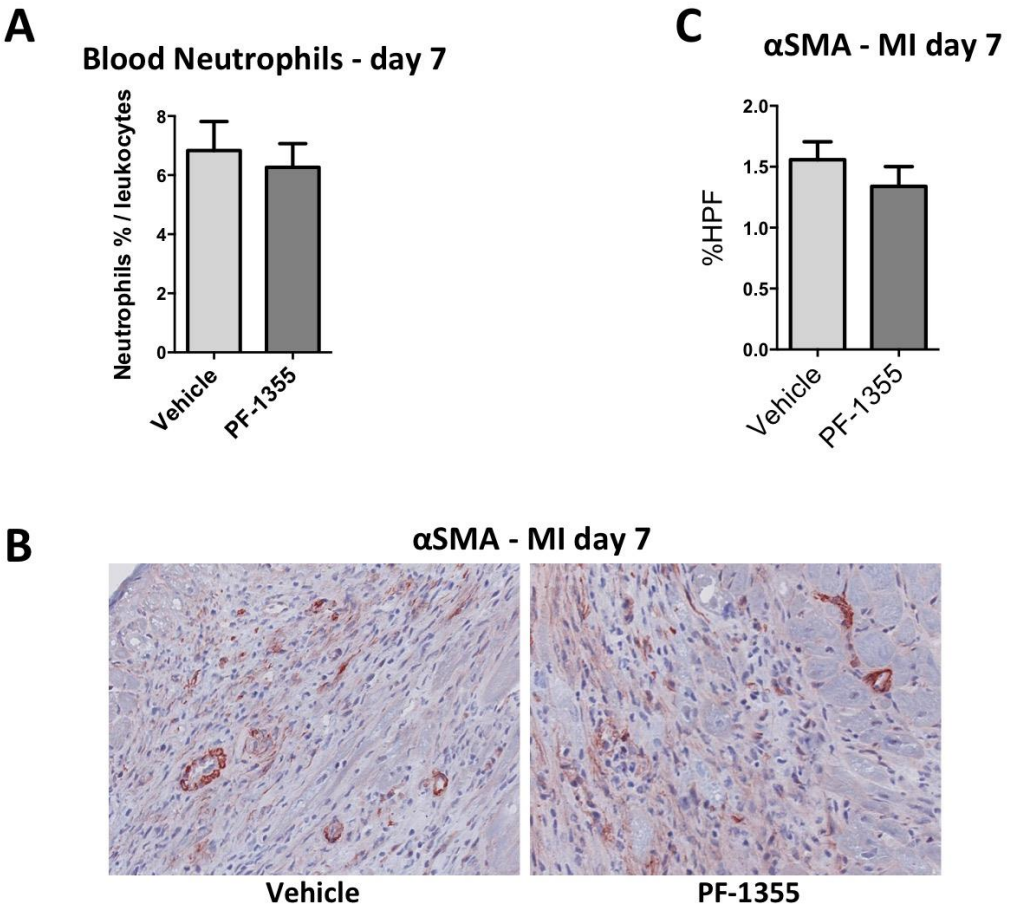

SI Fig. 4: (A) PF-1355 treatment preserved neutrophil percentages in the blood at day 7 after MI induction (p=0.66, n=4-5/group). **(B&C)** αSMA immunohistochemistry plotted as percentage of high power field (% HPF) was also similar between vehicle and PF-1355 treated groups (p=0.35, n=5). Data plotted as mean ± SEM

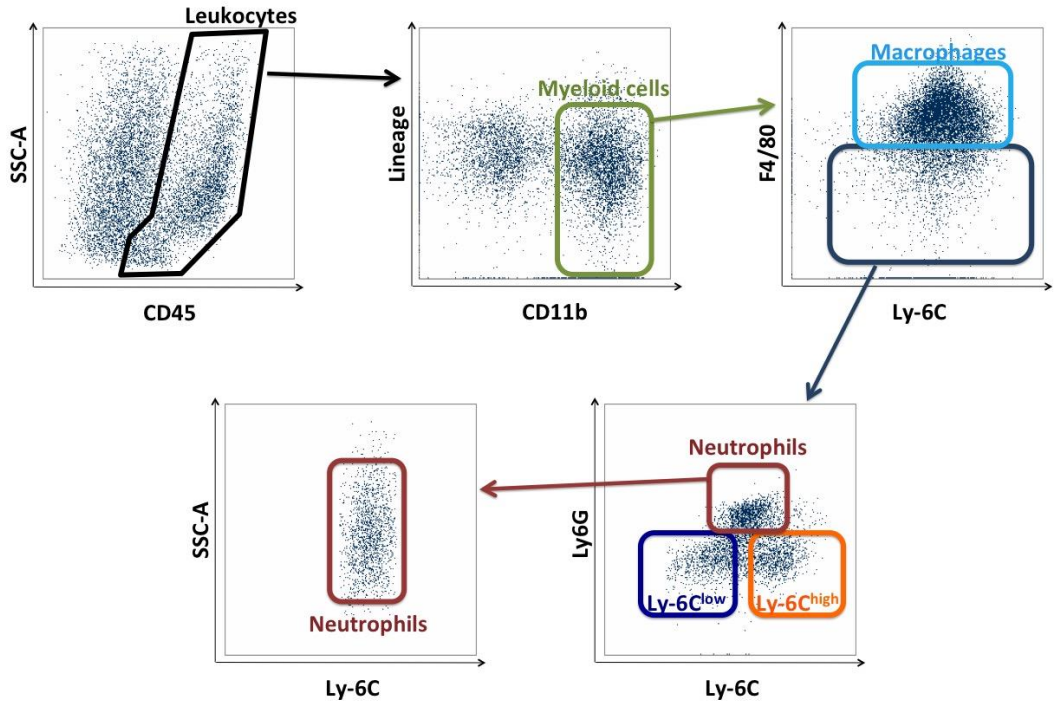

SI Fig. 5: Gating strategy for the leukocyte extracts from cardiac infarct tissue isolated at day 15. Live cells were identified and doublets were excluded with the help of forward and side scatter gates (not shown). Leukocytes were identified as $CD45^{+}$ (Black gate) while $CD11b^{+}$ cells (myeloid cells; green box) as $(CD45^{+})(Lin^{low}\ CD11b^{high})$. From the CD11b positive gate, macrophages were identified as $F4/80^{high}$ (light blue box), neutrophils (red box) as $[(F4/80^{low})(Ly\text{-}6G^{high}\ Ly\text{-}6C^{int})(SSC^{int\text{-}high})]$, and monocytes either as $Ly\text{-}6C^{high}$ monocytes [orange box; $(F4/80^{low})(Ly\text{-}6G^{low}\ Ly\text{-}6C^{high})$] or $Ly\text{-}6C^{low}$ monocytes [dark blue box; $(F4/80^{low})(Ly\text{-}6G^{low}\ Ly6C^{low})$].